Chinese Journal of
POLYMER SCIENCE 高分子科学

Top-down Approach for Fabrication of Polymer Microspheres by Interfacial Engineering

Fan Yue, Wang De-Hui, Yang Jin-Long, Song Jia-Ning, Li Xiao-Mei, Zhang Cheng-Lin, Wang Dong-Sheng, Chen Long-Quan, Cui Jia-Xi, Deng Xu

Cite this article as:
Fan Yue, Wang De-Hui, Yang Jin-Long, Song Jia-Ning, Li Xiao-Mei, Zhang Cheng-Lin, Wang Dong-Sheng, Chen Long-Quan, Cui Jia-Xi, Deng Xu. Top-down Approach for Fabrication of Polymer Microspheres by Interfacial Engineering[J]. *Chinese J. Polym. Sci*, In press. doi: 10.1007/s10118-020-2453-3

View online: https://doi.org/10.1007/s10118-020-2453-3

Articles you may be interested in

Design and Fabrication of Functional Hydrogels through Interfacial Engineering
Chinese J. Polym. Sci. 2017, 35(10): 1181 https://doi.org/10.1007/s10118-017-1995-5

Preparation of Porous Polylactide Microspheres and Their Application in Tissue Engineering
Chinese J. Polym. Sci. 2018, 36(6): 712 https://doi.org/10.1007/s10118-018-2079-x

FUNCTIONALIZING PS MICROSPHERES BY SUPERCRITICAL DEPOSITION OF P(S-b-tBA) FOR DIVERSE INTERFACIAL PROPERTIES EXEMPLIFIED WITH BIOCIDAL ABILITY
Chinese J. Polym. Sci. 2012, 30(3): 451 https://doi.org/10.1007/s10118-012-1136-0

P(St-AM)核壳聚合物微球的制备及其光子晶体膜
FABRICATION OF CORE-SHELL POLYMER MICROSPHERES OF P(St-AM) AND THE CORRESPONDING PHOTONIC CRYSTALS FILMS
高分子学报. 2012(6): 648 https://doi.org/10.3724/SP.J.1105.2012.11334

聚己二酸丁二酯纳米纤维构建的微球的制备
FABRICATION OF POLY(BUTYLENE ADIPATE) NANOFIBEROUS MICROSPHERES
高分子学报. 2013(6): 781 https://doi.org/10.3724/SP.J.1105.2013.13043

不良溶剂氛围中用 breath figures 法制备聚合物微球
Fabrication of Polymeric Microspheres by Breath Figures in Different Nonsolvent Atmospheres
高分子学报. 2014(12): 1606 https://doi.org/10.11777/j.issn1000-3304.2014.14109

Chinese Journal of
POLYMER SCIENCE

ARTICLE

https://doi.org/10.1007/s10118-020-2453-3
Chinese J. Polym. Sci.

Top-down Approach for Fabrication of Polymer Microspheres by Interfacial Engineering

Yue Fan[a], De-Hui Wang[a], Jin-Long Yang[a], Jia-Ning Song[a], Xiao-Mei Li[b], Cheng-Lin Zhang[a], Dong-Sheng Wang[c*], Long-Quan Chen[d], Jia-Xi Cui[a], and Xu Deng[a*]

[a] *Institute of Fundamental and Frontier Sciences, University of Electronic Science and Technology of China, Chengdu 610054, China*
[b] *Department of Physics at Interfaces, Max Planck Institute for Polymer Research, Ackermannweg 10, 55128, Mainz, Germany*
[c] *School of Optoelectronic Science and Engineering, University of Electronic Science and Technology of China, Chengdu 610054, China*
[d] *School of Physics, University of Electronic Science and Technology of China, Chengdu 610054, China*

Electronic Supplementary Information

Abstract Polymer microspheres with uniform size, composition, and surface property have gained extensive researches in past decades. Conventional bottom-up approaches are using monomers or oligomers to build up desired polymer microspheres. However, directly shaping high-molecular-weight polymers into well-ordered polymer microspheres remains a great challenge. Herein, we reported a facile and efficient top-down approach to fabricate microspheres with high-molecular-weight polymer microfibers. By harnessing interfacial engineering-control during the polymer microspheres formation, uniformly sized microspheres could be produced with widely ranged diameters (from 10 μm to the capillary length of each polymer melt). The size limitation of this approach could be further extended by a controllable Plateau-Rayleigh instability phenomenon. Principally, the top-down approach allows fabrication of microspheres by various polymer melts with surface energy higher than 25 mN/m. Our work paves a way for green, cost-effective, and customizable production of a variety of functional polymer microspheres without any chemical reaction assistant.

Keywords Superamphiphobic surfaces; Microfluidic spinning; Microfibers; Microspheres

Citation: Fan, Y.; Wang, D. H.; Yang, J. L.; Song, J. N.; Li, X. M.; Zhang, C. L.; Wang, D. S.; Chen, L. Q.; Cui, J. X.; Deng, X. Top-down approach for fabrication of polymer microspheres by interfacial engineering. *Chinese J. Polym. Sci.* https://doi.org/10.1007/s10118-020-2453-3

INTRODUCTION

For decades, polymer microspheres have received widespread concerns for the characteristics of micron scale, spherical structure, size uniformity, and great specific surface area. With these characteristics, practical applications in various fields can be achieved such as drug delivery,[1–3] chemical sensing,[4,5] materials modification,[6,7] and imaging.[8] Till now, plenty of researches have been reported on synthesizing and controlling the constituents, structures, sizes, and properties of polymer microspheres.

Conventional methods for producing polymer microspheres employed bottom-up strategies, for instance chemical synthesis, including dispersion, seed, emulsion, and mini-emulsion polymerizations.[9–12] To achieve polymer microspheres with various structures and sizes, the conditions during polymerization (*e.g.* monomers, organic solvents, emulsifiers, and surfactants) need to be controlled carefully. Recently, several bottom-up strategies were reported to produce polymer microspheres with physical methods, such as microfluidic technique and evaporation.[13,14]

However, the bottom-up strategies are difficult to cover all the requirements. For instance, the polymer sphere lens and micro-spacers in precision instruments require that the existing polymer bulk can be directly shaped into microspheres. Although the current 3D micro-printing technology can produce desired objects at the micro-scale resolution, it is highly costly and difficult to achieve spherical morphology. The micro-injection also remains a challenge to produce polymer microspheres with desired structures and sizes. Therefore, seeking for a top-down approach to fabricate microspheres directly by high-molecular-weight polymers ($M_w > 1 \times 10^5$) is urgent and necessary.

In contrast with the conventional bottom-up strategies to synthesize polymer microspheres through chemical reactions, we herein reported a top-down strategy fabricating microspheres directly by high-molecular-weight polymer microfibers on superamphiphobic surfaces, where neither template nor mold assistant was needed. Although methods mentioned above have been reported to prepare microspheres without a template (*e.g.* dispersion and emulsion

* Corresponding authors, E-mail: wangds@uestc.edu.cn (D.S.W.)
E-mail: dengxu@uestc.edu.cn (X.D.)

Received March 8, 2020; Accepted May 6, 2020; Published online July 17, 2020

© Chinese Chemical Society
Institute of Chemistry, Chinese Academy of Sciences
Springer-Verlag GmbH Germany, part of Springer Nature 2020

polymerization, 3D micro-printing technology), our work provided a rarely developed route on the basis of interfacial engineering.[15–21] Template-free method was also reported in our previous work,[22] where polymer powders were used to produce microshperes on superamphiphobic surfaces. However, it was difficult to prepare microspheres with continuously tunable and uniform sizes with the previous strategy. In our current method, patterned microfibers with desired length were first prepared on superamphiphobic surfaces *via* microfluidic spinning and laser cutting technology; after annealing the patterned microfibers at a temperature above the viscous flow temperature (T_f), the interfacial tension induced microfiber melt to be shaped into spherical structures; ultimately, polymer microspheres could be produced after cooling. Without mass use of organic solvents and costly devices, our process tended to be eco-friendly and cost-effective. The sizes of the microspheres were uniform and well-tunable by controlling the diameters and lengths of the patterned microfibers. The microsphere diameters could be tuned between 10 μm and the capillary length of each polymer melt. Furthermore, we can extend the size scale of microspheres to an order of magnitude more (1–10 μm diameters) by the controllable Plateau-Rayleigh instability (PRI) phenomenon of the microfiber melts on superamphiphobic surfaces.[23–26] We envision this novel top-down strategy can be used as a universal method for shaping various bulk polymer or polymer composite into microspheres.

EXPERIMENTAL

Materials

Poly(methyl methacrylate) (M_w = 1.2 × 10^5 g/mol, Sigma-Aldrich), *N*,*N*-dimethylformamide (AR, 99.5%, Aladdin), ammonia solution (28% in water, TCI), tetraethoxysilane (TEOS, 98%, Sigma-Aldrich), trichloro(1*H*,1*H*,2*H*,2*H*-perfluorooctyl)silane (Sigma Aldrich), and hexadecane (AR, 98%, Aladdin) were used as purchased without purification. Glass slides (30 mm × 30 mm × 0.17 mm) were bought from Marienfeld. The deionized water was purified by a Millipore water purification system which has a minimum resistivity of 18.0 MΩ·cm.

Preparation of Superamphiphobic Surfaces

Firstly, taking a glass slide (30 mm × 30 mm × 0.17 mm) as the substrate, a black and uniform candle soot layer was generated by holding and moving the glass slide in the flame of a burning candle. The collection time for individual glass slide was ~2 min. Secondly, the soot-coated glasses were transferred to a desiccator. Two open glass vessels were placed in the desiccator as well, containing 4 mL of tetraethoxysilane and 4 mL of aqueous ammonia solution, respectively. By vacuuming the desiccator, the Stöber reaction occurred on the glass surface. The chemical vapor deposition was carried out for ~24 h. Thirdly, oxygen plasma was used to treat the sample for 10 min. Then, the samples were transferred to a desiccator again together with an open glass vessel of 200 μL trichloro(1*H*,1*H*,2*H*,2*H*-perfluorooctyl)silane. The desiccator was then vacuumed to a pressure of 0.01 MPa and kept for 2 h. After that, the superamphiphobic surfaces were taken out from the desiccator, and the desiccator experienced the fullness of nitrogen gas and vacuum for several times, to remove the residual silane.

Fabrication of Ordered Microfibers on Superamphiphobic Surfaces

A microfluidic-spinning setup consisting of a rotor, a syringe pump, and a stepping device (Nanjing Janus New Materials Co., Ltd.) was used to prepare the ordered microfibers on superamphiphobic surfaces. Take PMMA as the example. During the preparation step, a superamphiphobic glass slide was clamped on the rotor and 30 wt% PMMA/DMF solution was put in the syringe. During the microfiber fabrication step, the rotor, syringe pump, and stepping device were manipulated simultaneously, with 80 r/min rotating speed, 0.05 mL/min pumping speed, and 2 mm/s stepping rate, respectively. The ordered PMMA microfibers were then collected on the superamphiphobic surface with uniform spacing. Besides, the microfibers with tunable sizes and spacings could be achieved by tuning the rotating speed, pumping speed, and stepping rate.

Preparation of Patterned Microfibers

Take PMMA as the example. The glass slides with ordered PMMA microfibers were placed on a three-dimensional (3D) electric displacement platform. Then a silicon mask with a ~15 μm gap was put on the ordered microfibers with a distance less than 1 mm. The orientation of the gap should be perpendicular to the orientation of microfibers. After that, an infrared laser (wavelength = 808 nm, power ~1 W) was set to focus on a point of the gap. The microfibers were cut when a relative motion was controlled between the glass slide and the infrared laser with a speed of 50 mm/s. After cutting the microfibers repeatedly, PMMA patterned microfibers were generated on the superamphiphobic surface. Moreover, microfibers could be cut into various lengths by tuning the space of laser cutting.

Fabrication of Microspheres

We utilized a heating stage (LTSE420, Linkam Scientific) to generate microspheres from patterned microfibers. Take PMMA as the example. The superamphiphobic glass slide with PMMA patterned microfibers was put on the heating stage. With a heating rate of 30 °C/min, the temperature of the heating stage chamber was raised to 180 °C. Then the temperature was kept at 180 °C until the PMMA patterned microfibers transformed into microsphere melts completely. PMMA microspheres could be achieved after natural air cooling.

Characterization

The optical micrographs and video microscope images of the samples were obtained by an industrial microscope (NIKON, LV100ND). Static contact angle measurements of the surfaces were performed at ambient temperature by a Contact Angle system OCA (DataPhysics Instruments), applying the sessile drop method. The morphology of the superamphiphobic surface and microspheres was investigated with a scanning electron microscope (SEM, Phenom ProX). The samples were coated with a 10 nm gold layer by using a sputter coater (IXRF Systems). Interface status between the microsphere and the surface was monitored utilizing an inverted laser scanning confocal microscope (Nikon, A1R).

RESULTS AND DISCUSSION

The top-down approach to prepare polymer microspheres was divided into three stages: (i) preparing ordered polymer

https://doi.org/10.1007/s10118-020-2453-3

microfibers on superamphiphobic surfaces (stage I), (ii) processing patterned microfibers by laser cutting (stage II), (iii) producing polymer microspheres on superamphiphobic surfaces by thermally annealing patterned microfibers (stage III).

In stage I, we first prepared superamphiphobic surfaces based on a fractal-like arrangement of candle soot particles (Fig. 1a, see detail in section 2 of the electronic supplementary information, ESI).[27–29] On superamphiphobic surfaces, liquid with surface tension higher than 25 mN/m showed the apparent contact angles above 150° in the air, such as water, organic solvent, and even polymer solutions (Fig. S1 in ESI). For instance, poly(methyl methacrylate) (PMMA, M_w = 1.2 × 10^5 g/mol) solution in *N*,*N*-dimethylformamide (DMF) (30 wt%) showed a 152° contact angle on this surface, trapping air beneath PMMA solution and preserving the solution in a Cassie state (Fig. 1b). Distinct from water and organic solvent, polymer solutions revealed much greater adhesion force on superamphiphobic surfaces, which contributes to the stability of microfiber arrays on superamphiphobic surfaces (Fig. 1c, see detail in ESI, section 3). A microfluidic-spinning setup was then utilized to fabricate ordered polymer microfibers on the superamphiphobic surfaces (Fig. 1d). Microfluidic-spinning technology showed superiorities in effective control of the categories, sizes, and spacings of polymer microfibers.[30–32] In principle, thermoplastic polymers with surface tension higher than 25 mN/m can be used to fabricate microspheres by this method only if they are spinnable. Some appropriate contents of polymer spinning solution and the surface tensions of polymers at different temperatures are shown in Tables S1 and S2 (in ESI). PMMA was selected as the prototype material for microfiber fabrication because it has suitable glass-transition temperature (T_g = 105 °C) and excellent spinnability.[30] It is also a common model exhibited in various methods to prepare microspheres, such as dispersion polymerization,[9] seed polymerization,[33] and membrane emulsification.[34] Regular and uniform PMMA microfibers were fabricated by 30 wt% PMMA solution in DMF (Fig. 1e). Besides, by adjusting related parameters of microfluidic-spinning setup, the microfibers with tunable sizes and spacings could be achieved (Figs. S2 and S3 in ESI). Narrow size distribution of ordered PMMA microfibers with the selected diameters of 3, 5, and 7 μm was demonstrated, indicating that with this method ordered and uniform polymer microfibers could be fabricated (Fig. 1f).

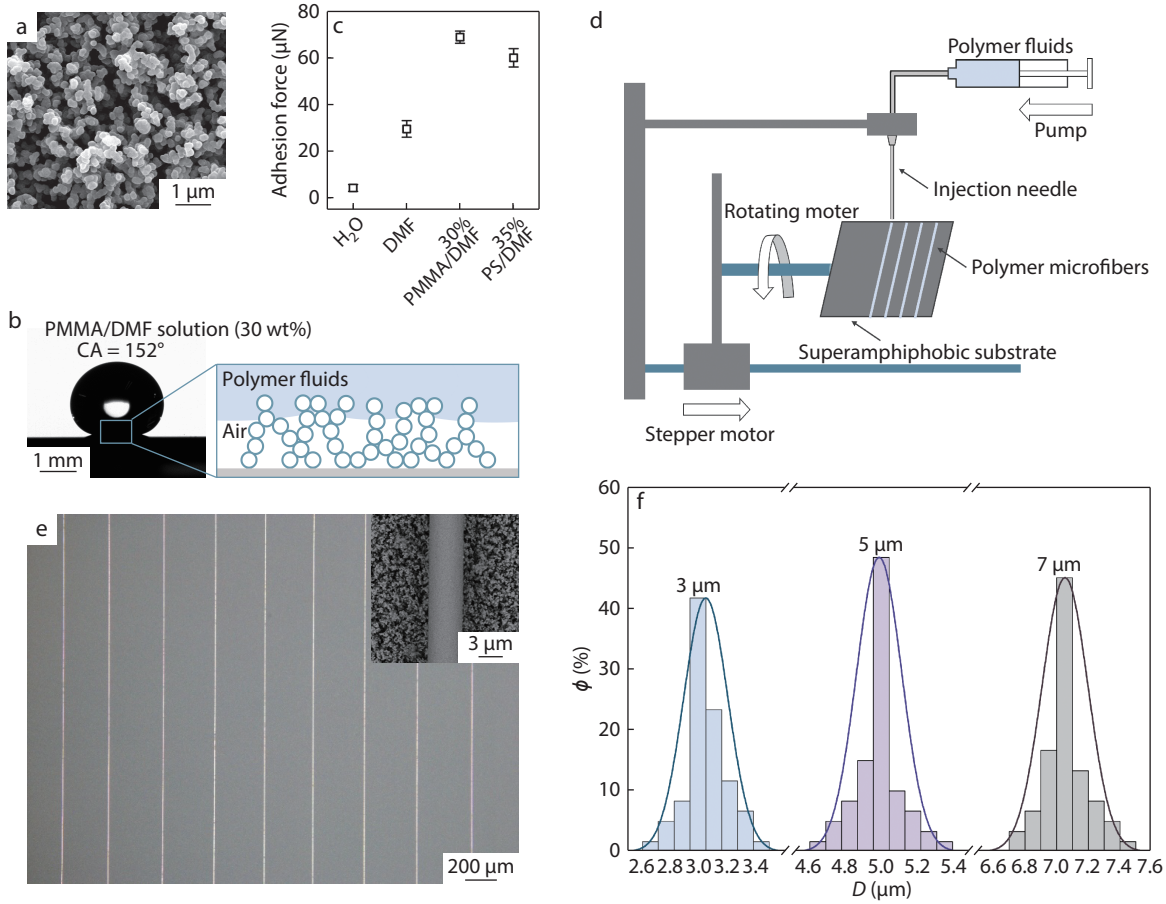


Fig. 1 Designing ordered polymer microfibers on superamphiphobic surfaces: (a) SEM image of the superamphiphobic surface; (b) contact angle of 30 wt% PMMA/DMF solution on the superamphiphobic surface; (c) adhesion forces of droplets (8 μL) on the superamphiphobic surface; (d) schematic illustration of the microfluidic-spinning setup for designing ordered microfibers on the superamphiphobic surface; (e) optical micrographic image of PMMA microfibers arrays on the superamphiphobic surface (the inset shows the SEM image of a single microfiber); (f) the size distribution of ordered PMMA microfibers fabricated in selected diameters of 3, 5, and 7 μm.

https://doi.org/10.1007/s10118-020-2453-3

Based on the controllable fabrication of ordered polymer microfibers, in stage II, a set of laser cutting experimental apparatus including a 3D electric displacement platform, a silicon mask, and an infrared laser (wavelength = 808 nm, power ~1 W) was established (Fig. 2a). A silicon mask with ~15 μm gap was prepared by photolithography (Fig. S4 in ESI), and was placed right onto the ordered microfibers with less than 1 mm distance. Thus, with relative movement between irradiation spot and ordered microfibers at a 50 mm/s speed, micron zone on each microfiber can be heated rapidly above the glass-transition temperature (T_g). As a result, an exact breakup at the irradiated zone of each microfiber occurred simultaneously, induced by the interaction between polymer chain motion in micro-level zone and surface tension of the whole microfiber. Therefore, by adjusting spacings between two laser spot motion tracks, patterned microfibers with desirable lengths could be fabricated, even with a gradually increasing length (Fig. S5 in ESI). For ordered PMMA microfibers with diameters of 4 ± 0.2 μm, patterned PMMA microfibers with equal length of ~650 μm were fabricated on the superamphiphobic surfaces (Fig. 2c).

Finally, due to the high fluid repellency of superamphiphobic surfaces,[27,35,36] polymer microspheres were fabricated by annealing the patterned microfibers above T_f (stage III) (Fig. 2b and Video S1 in ESI). Fig. 2(d) shows the optical micrographic image of PMMA microparticles produced by micropatterned microfibers in Fig. 2(c), demonstrating that the top-down approach was an *in situ* process to fabricate microspheres. Note that the fabricated PMMA microparticles maintained the spherical shape and smooth surface, and the microsphere fabricating process did not damage the superamphiphobic surface (Fig. 2e).

Interestingly, we observed a two-step process when microfibers were heated to generate microspheres. At the beginning stage of thermal treatment, especially when the temperature T was between T_g and T_f, microfibers were shrunk uniformly to kept a cylindrical shape with a decreased length as well as an increased column size (Fig. 3a). However, this trend of overall contraction stopped when microfibers reached T_f. In contrast, both ends of the microfiber melts started to generate spherical aggregations (Fig. 3a).

This phenomenon could be simply explained from the perspective of surface energy. Assuming two distinct states of microfiber melt (dumbbell shape and cylindrical structure) at an identical immediate temperature over T_f, there was an extra surface energy $\Delta E = \gamma_{ls}\Delta S_{ls} + \gamma_{lv}\Delta S_{lv}$ in cylindrical state of the microfiber melt (Fig. 3b, see detail in ESI section 8). The dumbbell state of the microfiber melt was thus more stable and favorable to be formed. Generally, by heating microfibers from room temperature to T_f at a suitable heating rate (*e.g.* 30 °C/min), these features were universally observed for microfibers with diverse materials and sizes.

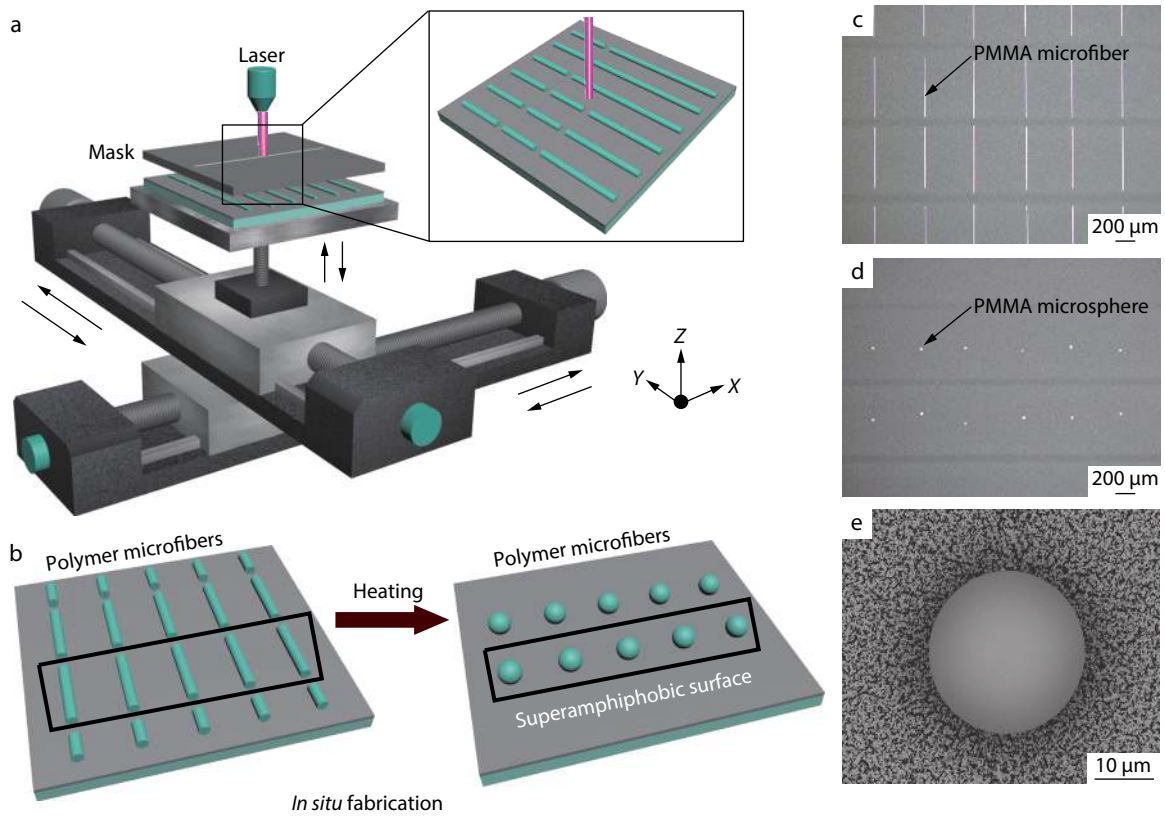


Fig. 2 Fabrication of microspheres by microfiber processing: (a) schematic illustration of the laser cutting setup (consisting of a 3D electric displacement platform, a silicon mask and an infrared laser) to design patterned microfibers; (b) schematic illustration of the thermal annealing process to *in situ* fabricate microspheres from patterned microfibers; (c) optical micrographic image of patterned PMMA microfibers on the superamphiphobic surfaces; (d) optical micrographic image of the fabricated PMMA microspheres from the patterned microfibers in Fig. 2(c); (e) SEM image of a fabricated PMMA microsphere.

https://doi.org/10.1007/s10118-020-2453-3

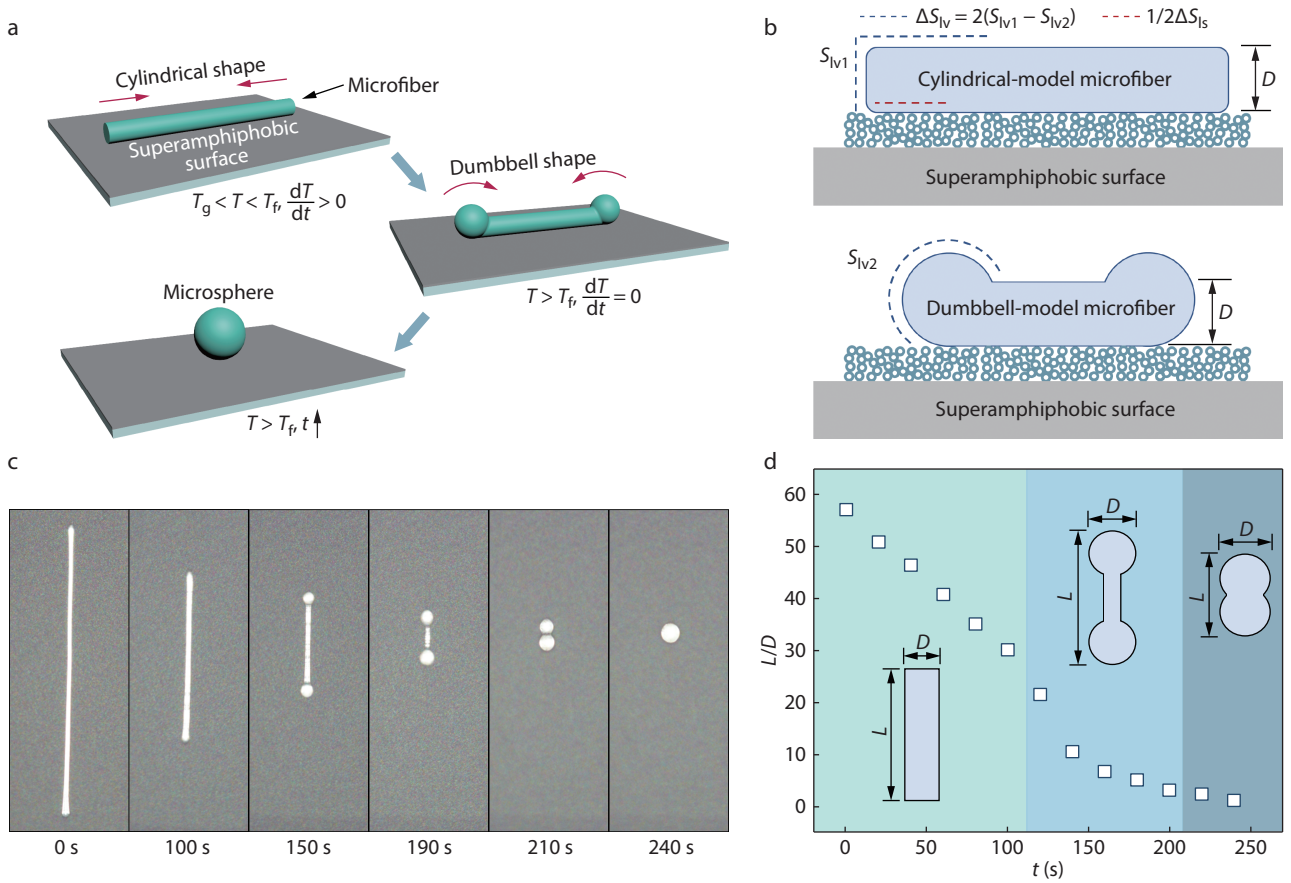


Fig. 3 Process of thermal treatment of microfibers on superamphiphobic surfaces: (a) schematic illustration of the intermediate phenomena in the process (d*T*/d*t* is the heating rate, *t*↑ represents the increase in time); (b) side views of microfiber melts with dumbbell shape and cylindrical structure to analyze the distinction in the surface energy; (c) sequence of video microscopic images of a PMMA microfiber heated to 180 °C on the superamphiphobic surface; (d) plot of length to diameter ratio (*L*/*D*) versus time of thermal treatment (*t*) to analyze the time-dependent microfibers shape transformation in the whole process.

We investigated the formation process of PMMA microspheres, with an initial temperature of 105 °C to the temperature of 180 °C at a 30 °C/min heating rate (Fig. 3c and Video S2 in ESI). The spherical aggregations were observed at 150 s, while the microspheres were generated in 240 s and preserved after cooling. The time-dependent shape transformation process was analyzed by a length to diameter ratio (*L*/*D*), where *L* is the length of microfiber and *D* is the section diameter in the ends of microfiber (Fig. 3d). Three configurations performed in the whole process could be clearly identified. Initially, the *L*/*D* ratio decreased almost linearly with time, suggesting that the microfiber remained shrinking uniformly. In the next nonlinear growth regime, the ratio experienced a sharp fall, signifying the gradually increased size of spherical aggregations in the ends of microfiber. At the later stage, the ratio declined slowly and eventually became 1:1, indicating that two spherical aggregations merged into a single microsphere.

To study the dynamics in the contraction process, we investigated the relationships between temperature and the processing parameters. The temperature was increased by 30 °C/min in the whole process. The *L*/*D* ratio kept decreasing throughout the whole heating process, which was getting faster when the polymer melts were in the dumbbell-shape state. The viscosity of the polymer melts kept decreasing with the increased temperature, which can be further evaluated by the Williams-Landel-Ferry equation.[37] The surface tension of the polymer melts was in an inverse proportion to the temperature, matching the Eötvös equation.[38] Besides, the interaction of the surface tension against the adhesion force was also considered. The contact area between the polymer melt and superamphiphobic surface was much smaller than the contraction area of the melt, indicating the effect of adhesion force was negligible compared with that of surface tension. Note that the contact area was decreased during contracting. This decrease can further accelerate the contraction process.

Despite the special process, the top-down approach allows fabricating polymer microspheres with tunable and uniform sizes. Theoretically, the relationship between fabricated microspheres and initial microfibers could be expressed by the following equation:

$$D_p = \sqrt[3]{\frac{3}{2} L_f \cdot D_f^2} \quad (1)$$

where D_p is the diameter of the microsphere, L_f and D_f are the length and the sectional diameter of the microfiber, respectively. A good consistency between experimental measurements and the theoretical curve was demonstrated over the

whole measuring span, documenting the effective control of the microparticle size by adjusting the parameters of microfiber flexibly (Fig. 4a).

By this method, the microspheres can be fabricated with the broad size range corresponding to three orders of magnitude from 10 μm to the capillary length of each polymer melt. Note that the capillary length showed the biggest diameter of a fluid keeping quasi-spherical on the surface. Denoting $\Delta\rho$ as the density difference between the two phases, γ as the surface tension, and g as the acceleration due to gravity, the capillary length κ^{-1} can be therefore calculated by $\kappa^{-1} = (\gamma/\Delta\rho g)^{1/2}$. Further increasing the size might generate particles with hemi-spherical shape for the dominant effect of gravity against the surface tension. Taking PMMA as an example, the biggest diameter of spherical PMMA particle was calculated to be ~1.6 mm. Therefore, the PMMA particles with diameters in three orders of magnitude can be fabricated (Fig. S6 in ESI).

The size uniformity of the fabricated microspheres is important to our method. Microspheres with the desired diameters of 20, 25, and 30 μm were fabricated, all of which showed narrow size distribution (Fig. 4b). Interestingly, the size uniformity was better for the microspheres with larger diameters. These indicate that the top-down method was of great value in controllable and uniform production of polymer microspheres with diameters of dozens of microns, which are difficult to achieve by conventional strategies.

The diameter of ~10 μm was the minimum size which could be reached by this method due to the device restriction. To further generate microspheres with smaller sizes, we exploited the PRI phenomenon to break up the microfiber melt spontaneously in the annealing process on superamphiphobic surfaces. By controlling this phenomenon, the size limitation of the microspheres could be extended to one order of magnitude smaller (10^0 μm level), while the tunable microspheres sizes and uniformity were maintained.

The three-dimensional image of a fabricated microsphere on the superamphiphobic surface and its *X*-*Z* cross section were observed with the 3D confocal microscopy (Fig. 5a). Here we used a fluorescent polymer poly(styrene-*co*-HBA) labelled with rhodamine B (see detail of synthesis in ESI, section 10) to obtain the confocal image. With a measured contact angle of 158° and tiny actually contact area as well as no damage on the surface, polymer melt could be demonstrated to move freely on the superamphiphobic surface (Fig. 5a). These essentially make the PRI phenomenon possible to be happed on the superamphiphobi surface after external perturbations.

As the classical theory of the PRI phenomenon illustrated,[39] this process was dominated by the surface tension γ and could be described by a gradually increased pressure difference $\Delta P = \gamma(1/R_1 + 1/R_2)$ (the Young-Laplace equation,[40,41] R_1 and R_2 are the two principal radii of curvature). To investigate the variation process of the microfiber melt breaking up induced by the PRI effect, a PMMA microfiber (700 μm in length and 4 μm in diameter) was heated slowly (20 °C/min rate) to 220 °C (Fig. 5b and Video S3 in ESI). The initial perturbation occurred when the temperature reached 200 °C. After heating to 220 °C and annealing for 1.5 min, the

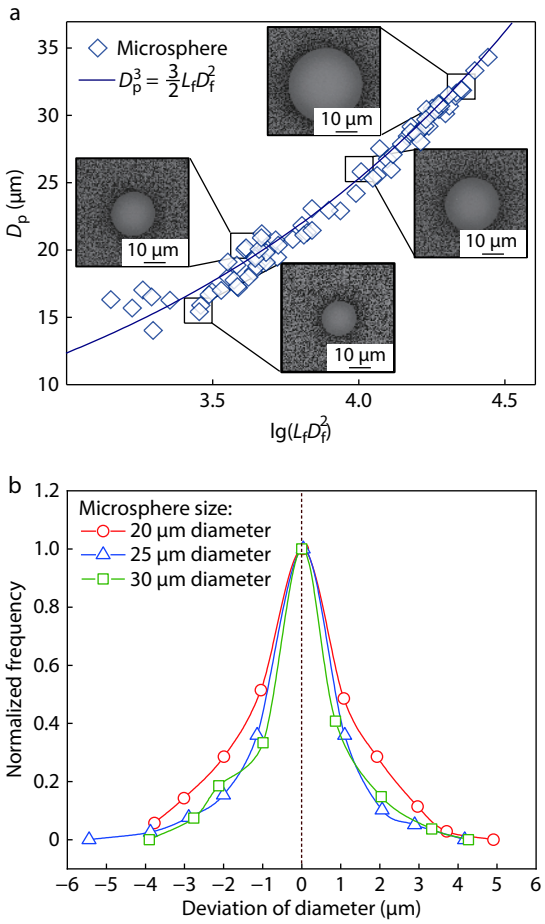


Fig. 4 Size control of microspheres fabricated by the top-down approach: (a) relation between diameters of microspheres (D_p) and parameters of microfibers (L_f and D_f are the length and diameter of the microfiber, respectively); (b) size distribution of three microsphere groups with average diameters of 20, 25, and 30 μm. The corresponding parameters of patterned microfibers were L_f ~350 μm, D_f ~4 μm (for 20 μm microspheres), L_f ~650 μm, D_f ~4 μm (for 25 μm microspheres), and L_f ~500 μm, D_f ~6 μm (for 30 μm microspheres).

bulged section and the pinched section were generated for the function of pressure gradient; after 2.5 min annealing, the breakup of the microfiber melt was observed at the pinched section. Finally, two microspheres were completely generated through a 5.5 min annealing totally.

Combining Tomotika linear stability theory with the PRI phenomenon of microfiber melts on superamphiphobic surfaces,[42] the length of microfiber and the annealing temperature are the key factors to affect the divided microspheres sizes (see detail in ESI, section 11). For example, a long microfiber with the length of 850 μm (also 4 μm in diameter) was annealed on the superamphiphobic surface at 240 °C (Fig. 5c). With sharp and multi-site perturbations, microspheres with the diameter of 6 μm could be fabricated, demonstrating that the microspheres with the size of 10^0 μm level are producible with the top-down method (Fig. 5c). We also draw a binary plot to reveal the effective control of PRI breakup (Fig. 5d). In the binary plot, the investigated microfibers were uniformly sized in diameter of 4 μm. It was

https://doi.org/10.1007/s10118-020-2453-3

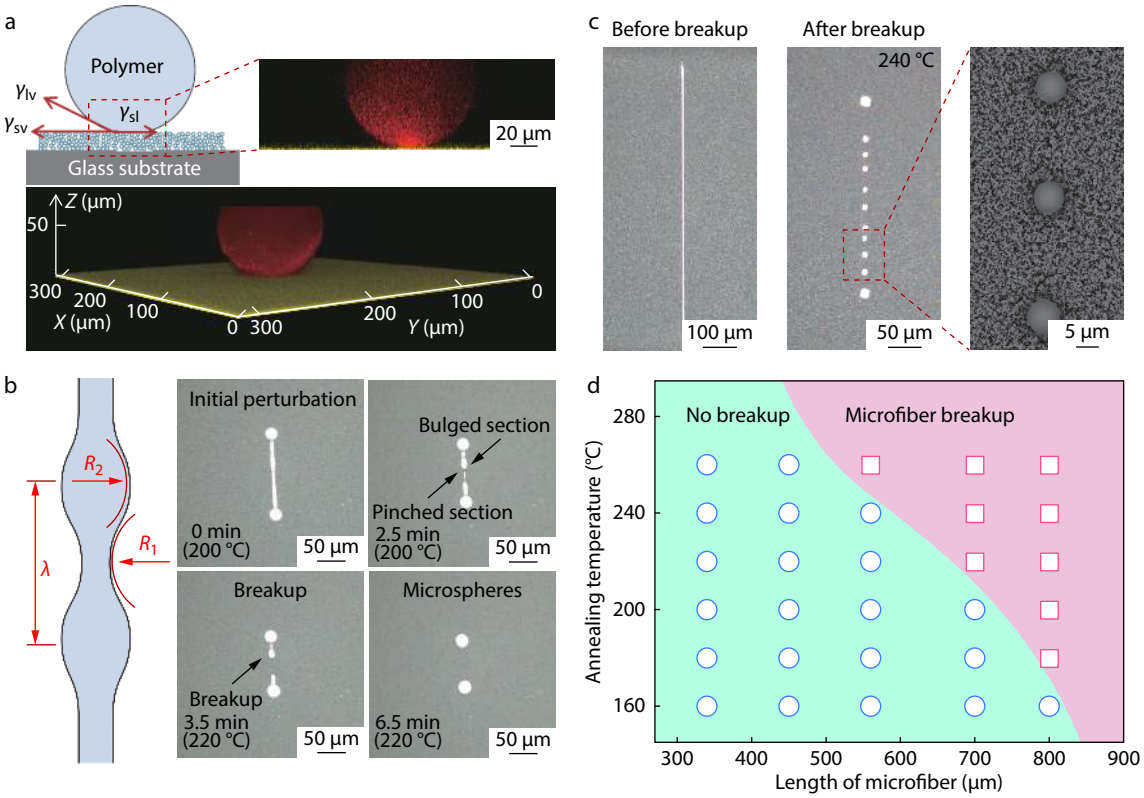


Fig. 5 Fabrication of microspheres with diameters of wider range induced by the PRI phenomenon on superamphiphobic surfaces: (a) three-dimensional confocal microscopic image and its *X*-*Z* cross section of a fluorescent polymer microsphere on the superamphiphobic surface; (b) the variation process of the PMMA melt breaking up into microspheres by the PRI phenomenon; (c) multi-site perturbations of a PMMA melt by the PRI phenomenon to produce microspheres with the size of 10^0 μm level in linear dimension; (d) the binary plot of annealing temperature versus microfiber length to analyze the borderline that differentiated the occurrence of microfiber melt breaking up spontaneously.

found that a borderline differentiated the occurrence of breakup, while multi-site perturbations could be achieved when an annealing temperature over the borderline was selected.

CONCLUSIONS

In summary, we proposed a new top-down approach to fabricate polymer microspheres by patterned microfibers on superamphiphobic surfaces. Three stages, (i) microfluidic-spinning polymer microfibers on superamphiphobic surface, (ii) cutting the microfibers into patterned microfibers, and (iii) heat annealing the patterned microfibers to fabricate polymer microspheres, are included in the fabricating process. Uniformly sized polymer microspheres could be well-controlledly prepared with the size range of three orders of magnitude in linear dimension from 10 μm to the capillary length of each polymer melt. Moreover, with a controllable PRI effect of microfiber melt, the size range of the microspheres might be extended to one more order of magnitude. In principle, this approach allows fabrication of polymer microspheres from various polymers with surface energy higher than 25 mN/m. We believe our method could greatly advance the next-generation strategies for fabrication of polymer microspheres which could outperform the majority of conventional approaches and suit to various of applications.

Electronic Supplementary Information

Electronic supplementary information (ESI) is available free of charge in the online version of this article.

ACKNOWLEDGMENTS

This work was financially supported by the National Natural Science Foundation of China (No. 21603026) and Sichuan Science and Technology Program (No. 2018RZ0115).

REFERENCES

1 Tibbitt, M. W.; Dahlman, J. E.; Langer, R. Emerging frontiers in drug delivery. *J. Am. Chem. Soc.* **2016**, *138*, 704–717.
2 Hossain, K. M. Z.; Patel, U.; Ahmed, I. Development of microspheres for biomedical applications: a review. *Prog. Biomater.* **2015**, *4*, 1–19.
3 Yang, F.; Niu, X.; Gu, X.; Xu, C.; Wang, W.; Fan, Y. Biodegradable magnesium-incorporated poly(L-lactic acid) microspheres for manipulation of drug release and alleviation of inflammatory response. *ACS Appl. Mater. Interfaces* **2019**, *11*, 23546–23557.
4 Salinas-Castillo, A.; Camprubi-Robles, M.; Mallavia, R. Synthesis of a new fluorescent conjugated polymer microsphere for chemical sensing in aqueous media. *Chem. Commun.* **2010**, *46*, 1263–1265.
5 Wei, W.; Lu, R.; Tang, S.; Liu, X. Highly cross-linked fluorescent

poly(cyclotriphosphazene-*co*-curcumin) microspheres for the selective detection of picric acid in solution phase. *J. Mater. Chem. A* **2015**, *3*, 4604–4611.
6 Duan, J.; Liang, X.; Guo, J.; Zhu, K.; Zhang, L. Ultra-stretchable and force-sensitive hydrogels reinforced with chitosan microspheres embedded in polymer networks. *Adv. Mater.* **2016**, *28*, 8037–8044.
7 Hou, J.; Ren, X.; Guan, S.; Duan, L.; Gao, G. H.; Kuai, Y.; Zhang, H. Rapidly recoverable, anti-fatigue, super-tough double-network hydrogels reinforced by macromolecular microspheres. *Soft Matter* **2017**, *13*, 1357–1363.
8 Cheng, K.; Yang, M.; Zhang, R.; Qin, C.; Su, X.; Cheng, Z. Hybrid nanotrimers for dual T_1 and T_2-weighted magnetic resonance imaging. *ACS Nano* **2014**, *8*, 9884–9896.
9 Zhang, X.; Cao, Y.; Jiang, Q.; Zhang, Y.; Yang, W. Preparation of cross-linked poly(methyl methacrylate) microspheres using an asymmetric cross-linker *via* dispersion polymerization and its application in light diffusers. *Colloid Polym. Sci.* **2020**, 1–10.
10 Kawaguchi, H. Functional polymer microspheres. *Prog. Polym. Sci.* **2000**, *25*, 1171–1210.
11 Wichaita, W.; Polpanich, D.; Tangboriboonrat, P. Review on synthesis of colloidal hollow particles and their applications. *Ind. Eng. Chem. Res.* **2019**, *58*, 20880–20901.
12 Liang, F.; Zhang, C.; Yang, Z. Rational design and synthesis of Janus composites. *Adv. Mater.* **2014**, *26*, 6944–6949.
13 Zhang, Y.; Cattrall, R. W.; Kolev, S. D. Fast and environmentally friendly microfluidic technique for the fabrication of polymer microspheres. *Langmuir* **2017**, *33*, 14691–14698.
14 Wooh, S.; Huesmann, H.; Tahir, M. N.; Paven, M.; Wichmann, K.; Vollmer, D.; Tremel, W.; Papadopoulos, P.; Butt, H. J. Synthesis of mesoporous supraparticles on superamphiphobic surfaces. *Adv. Mater.* **2015**, *27*, 7338–7343.
15 Zhan, K.; Hou, X. Tunable microscale porous systems with dynamic liquid interfaces. *Small* **2018**, *14*, 1703283.
16 Han, H.; Lee, J. S.; Kim, H.; Shin, S.; Lee, J.; Kim, J.; Hou, X.; Cho, S.W.; Seo, J.; Lee, T. Single-droplet multiplex bioassay on a robust and stretchable extreme wetting substrate through vacuum-based droplet manipulation. *ACS Nano* **2018**, *12*, 932–941.
17 Min, L.; Zhang, H.; Pan, H.; Wu, F.; Hu, Y.; Sheng, Z.; Wang, M.; Zhang, M.; Wang, S.; Chen, X. Controllable liquid-liquid printing with defect-free, corrosion-resistance, unrestricted wetting condition. *iScience* **2019**, *19*, 93–100.
18 El-Ballouli, A. O.; Bakr, O. M.; Mohammed, O. F. Compositional, processing, and interfacial engineering of nanocrystal- and quantum-dot-based perovskite solar cells. *Chem. Mater.* **2019**, *31*, 6387–6411.
19 Wang, S.; Yang, X.; Wu, F.; Min, L.; Chen, X.; Hou, X. Inner surface design of functional microchannels for microscale flow control. *Small* **2020**, *16*, 1905318.
20 Ju, J.; Yao, X.; Hou, X.; Liu, Q.; Zhang, Y. S.; Khademhosseini, A. A highly stretchable and robust non-fluorinated superhydrophobic surface. *J. Mater. Chem. A* **2017**, *5*, 16273–16280.
21 Cai, C.; Dauskardt, R. H. Nanoscale interfacial engineering for flexible barrier films. *Nano Lett.* **2015**, *15*, 6751–6755.
22 Deng, X.; Paven, M.; Papadopoulos, P.; Ye, M.; Wu, S.; Schuster, T.; Klapper, M.; Vollmer, D.; Butt, H. J. Solvent-free synthesis of microparticles on superamphiphobic surfaces. *Angew. Chem. Int. Ed.* **2013**, *52*, 11286–11289.
23 Kaufman, J. J.; Tao, G.; Shabahang, S.; Banaei, E. H.; Deng, D. S.; Liang, X.; Johnson, S. G.; Fink, Y.; Abouraddy, A. F. Structured spheres generated by an in-fibre fluid instability. *Nature* **2012**, *487*, 463–467.
24 Kaufman, J. J.; Ottman, R.; Tao, G.; Shabahang, S.; Banaei, E. H.; Liang, X.; Johnson, S. G.; Fink, Y.; Chakrabarti, R.; Abouraddy, A. F. In-fiber production of polymeric particles for biosensing and encapsulation. *Proc. Natl. Acad. Sci. USA* **2013**, *110*, 15549–15554.
25 Kuo, T. Y.; Tseng, H. F.; Chiu, Y. J.; Chen, J. T. Morphology transformations of electrospun polymer fibers annealed on polymer films with thickness-controlled growth rates of undulation. *Polymer* **2018**, *134*, 181–186.
26 Du, M.; Ye, S.; Tang, J.; Lv, S.; Chen, J.; Orava, J.; Tao, G.; Lan, P.; Hao, J.; Yang, Z.; Qiu, J.; Zhou, S. Scalable in-fiber manufacture of functional composite particles. *ACS Nano* **2018**, *12*, 11130–11138.
27 Deng, X.; Mammen, L.; Butt, H. J.; Vollmer, D. Candle soot as a template for a transparent robust superamphiphobic coating. *Science* **2012**, *335*, 67–70.
28 Schlaich, C.; Fan, Y.; Dey, P.; Cui, J.; Wei, Q.; Haag, R.; Deng, X. Universal, surfactant-free preparation of hydrogel beads on superamphiphobic and slippery surfaces. *Adv. Mater. Interfaces* **2018**, *5*, 1701536.
29 Li, X.; Wang, D.; Tan, Y.; Yang, J.; Deng, X. Designing transparent micro/nano re-entrant-coordinated superamphiphobic surfaces with ultralow solid/liquid adhesion. *ACS Appl. Mater. Interfaces* **2019**, *11*, 29458–29465.
30 Du, X. Y.; Li, Q.; Wu, G.; Chen, S. Multifunctional micro/nanoscale fibers based on microfluidic spinning technology. *Adv. Mater.* **2019**, *31*, 1903733.
31 Xu, L. L.; Wang, C. F.; Chen, S. Microarrays formed by microfluidic spinning as multidimensional microreactors. *Angew. Chem. Int. Ed.* **2014**, *53*, 3988–3992.
32 Zhang, Y.; Wang, C. F.; Chen, L.; Chen, S.; Ryan, A. J. Microfluidic-spinning-directed microreactors toward generation of multiple nanocrystals loaded anisotropic fluorescent microfibers. *Adv. Funct. Mater.* **2015**, *25*, 7253–7262.
33 Yu, B.; Xue, T.; Pang, L.; Zhang, X.; Shen, Y.; Cong, H. The effect of different porogens on porous PMMA microspheres by seed swelling polymerization and its application in high-performance liquid chromatography. *Materials* **2018**, *11*, 705.
34 Bux, J.; Manga, M. S.; Hunter, T. N.; Biggs, S. Manufacture of poly(methyl methacrylate) microspheres using membrane emulsification. *Philos. T. R. Soc. A* **2016**, *374*, 20150134.
35 Papadopoulos, P.; Vollmer, D.; Butt, H. J. Long-term repellency of liquids by superoleophobic surfaces. *Phys. Rev. Lett.* **2016**, *117*, 046102.
36 Zhao, B.; Wang, X.; Zhang, K.; Chen, L.; Deng, X. Impact of viscous droplets on superamphiphobic surfaces. *Langmuir* **2016**, *33*, 144–151.
37 Williams, M. L.; Landel, R. F.; Ferry, J. D. The temperature dependence of relaxation mechanisms in amorphous polymers and other glass-forming liquids. *J. Am. Chem. Soc.* **1955**, *77*, 3701–3707.
38 Shereshefsky, J. Surface tension of saturated vapors and the equation of Eötvös. *J. Phys. Chem.* **2002**, *35*, 1712–1720.
39 Rayleigh, L. XVI. On the instability of a cylinder of viscous liquid under capillary force. *Philos. Mag.* **1892**, *34*, 145–154.
40 Young, T. III. An essay on the cohesion of fluids. *Philos. Trans. R. Soc. London* **1805**, 95, 65–87.
41 Laplace, P. S. *Traité de mécanique céleste*. de l'Imprimerie de Crapelet: **1799**; Vol. 1.
42 Tomotika, S. On the instability of a cylindrical thread of a viscous liquid surrounded by another viscous fluid. *Proc. R. Soc. London, Ser. A* **1935**, *150*, 322–337.

https://doi.org/10.1007/s10118-020-2453-3